Available online at www.sciencedirect.com

ScienceDirect

Carbohydrate Polymers 72 (2008) 128–132

Carbohydrate Polymers

www.elsevier.com/locate/carbpol

Studies on the photocatalytic performance of cuprous oxide/chitosan nanocomposites activated by visible light

Jin-Yi Chen [a,b], Pei-Jiang Zhou [a,*], Jia-Lin Li [b], Yan Wang [b]

[a] *College of Resources and Environmental Sciences of Wuhan University, Wuhan 430079, PR China*
[b] *Nanotechnology Research Institute of Central China Normal University, Wuhan 430079, PR China*

Received 11 January 2007; received in revised form 26 July 2007; accepted 27 July 2007
Available online 10 August 2007

Abstract

Taking the chitosan nanoparticles prepared by adding only sodium sulfate into acetic acid solution of chitosan as carriers, cuprous oxide/chitosan nanocomposites were prepared by electrochemical deposition. It's found that the needle shaped cuprous oxide nanocrystallines are combined with chitosan particles by chelation. Activated by a visible light, Cu_2O/chitosan nanocomposites are used as a photocatalyst in the degradation of brilliant red X-3B of which the initial concentration is set as 50 mg/L. The results show that the best efficiency was obtained when the mass ratio of Cu_2O in Cu_2O/chitosan nanocomposites was 50%. And after the photocatalytic reaction, the residual copper element concentration can be cut down from 1.545 mg L^{-1} to 0.337 mg L^{-1} which is up to the drinking water standard of WHO.

Keywords: Electrochemical deposition; Nanocomposites; Photocatalysts; Cuprous oxide–chitosan; Visible light

1. Introduction

Cuprous oxide (Cu_2O) is a p-type semiconductor with a direct band gap of 2.0 eV(Yu, Du, Yu, Zhuang, & Wong, 2004), which is very important in hydrogen production, superconductors, solar cells, and negative electrode materials (Bohannan, Shumsky, & Switzer, 1999; Bordiga et al., 2001; Hara et al., 2000; Poizot, Laruelle, Grugeon, Dupront, & Taracon, 2000). As it can be activated by visible light, it has a potential application in photocatalytic degradation of organic pollutants under visible light (Jorge, Tetsuya, Jorge, Ortiz, & Sofía, 2001). Cu^+ deposited on zeolite has been used for the photocatalytic decomposition of NO_x into N_2 and O_2 (Anpo et al., 1998). And Cu_2O-activated carbon catalyst can decompose methanol to H_2 and CO directly (Tsoncheva, Nickdov, Vankova, & Mehandjiev, 2003). However, Cu_2O has not been commonly used because light-generated charge carriers in micronsized Cu_2O grains can not be efficiently transferred to the surface and are easy to be lost due to recombination, which results in low solar energy conversion efficiency (<1%) (Guido, Jacques, Michael, Nick, & Devendra, 1985; Tang, Chen, Jia, Zhang, & Li, 2005). At the same time, nano-sized Cu_2O particles reunite easily; and with respect to anodic photocorrosion, its stability is not so good. Therefore, the preparation of nanocrystalline Cu_2O materials is a key factor to improve the performance of solar energy. Moreover, the concentration of copper ions in water is a well-known issue which has to be controlled according to drinking water standard because although copper ions are essential micronutrients for human bodies, in large amounts of it (over 1.3 mg/L) (Marisa, Beppu, Arruda, Vieira, & Santos, 2004), humans may suffer from temporary stomach, intestinal disorders, and even kidney or liver damage depending on the time of exposure. The concentration of copper element produced by anodic photocorrosion is an important factor to hold back the application of nano-sized Cu_2O particles in decontamina-

---

[*] Corresponding author. Tel.: +86 27 87152823.
E-mail address: zhoupj@whu.edu.cn (P.-J. Zhou).

0144-8617/$ - see front matter © 2007 Elsevier Ltd. All rights reserved.
doi:10.1016/j.carbpol.2007.07.036

tion of wastewater as a semiconductor photocatalyst. Thus, selecting coating supports which can not only fix and disperse nano-sized Cu_2O particles, but also control the release of copper element produced into water is crucial for the application of Cu_2O to the decontamination of wastewater on a large scale. Several materials have been studied as supports, such as multiwall carbon nanotubes (Yu et al., 2005), active carbon (Chu, Lei, Hu, & Yue, 1998), glass substrate (Lu, Chen, & Lin, 2005), fiberglass (Jorge, Sergio, & Facundo, 2004), and polycarbonate membrane (Daltina, Addadb, & Chopart, 2005). But none of them have all the following properties: dispersing and fixing the nano-sized Cu_2O to prevent the recombination, chelateding copper element firmly by chelation and removing them from solution, a good sorbent to adsorb various pollutants, environmental and biologic compatibility, and cheap and abundant starting material.

Chitosan (CS), due to its hydrophilicity, chemical reactivity, moldability, mechanical properties, biocompatibility, and biodegradability, is an potential excellent material used in many areas such as food science, biochemistry, pharmaceuticals, medicine, agriculture, and so on (Sahidi, Arachchi, & Jeon, 1999; Vincendon, 1997). And owing to its unique three-dimensional structure of molecules, it exhibits an excellent capability to remove Cu(II) ions from aqueous solution by chelating (Guzman, Saucedo, Revilla, Navarro, & Guibal, 2003; Steenkamp, Keizer, Neomagus, & Krieg, 2002).

The main purpose of this paper was to select a feasible carrier to synthesize a new nanocomposite of Cu_2O in order to improve the photocatalytic performance and eliminate the copper element in the solution resulting from the Cu_2O nanocrystal during the photocatalytic degradation of pollutants. Based on our earlier findings with the growth mechanism of Cu_2O/CS nanoparticles (Chen, Zhou, Li, & Li, 2007), we have prepared different morphologies of Cu_2O nanoparticles on the surfaces of CS particles using a simple electrochemical approach. In the present report, we further examined the important photocatalytic performance of Cu_2O/CS nanocomposites used as a semiconductor photocatalyst for the degradation of dye X-3B with visible light irradiation. The disappearance of X-3B by different mass ratio of Cu_2O in the Cu_2O/CS composites under a visible light irradiation at $\lambda = 400$–800 nm were investigated. Finally, we compared the concentration of the copper element in the solution after photocatalysis reaction with different mass ratio of Cu_2O and Cu_2O/CS by ICP-AES.

2. Experiment

Chitosan was dissolved at 1% (w/v) with 1% (v/v) HOAc under magnetic stirring. Chitosan nanoparticles formed spontaneously upon addition of 10 mL 20% (w/v) Na_2SO_4 aqueous solution to chitosan solution under magnetic stirring. Nanoparticles were purified by centrifugation for 30 min. Supernatants were discarded, and the chitosan nanoparticles were extensively rinsed with distilled water to remove any sodium hydroxide and then dried in vacuum drying oven for 2 h at 333 K before further use or analysis. Cu_2O/CS nanoparticles were obtained by adding the chitosan nanoparticle into the anodic bath of an electrolytic cell designed by ourselves (Li et al., 2004). The anodic electrolyte was an aqueous solution of 300 g L^{-1} sodium chloride and the anode was a piece of copper sheet. The cathodal electrolyte was an aqueous solution of sodium hydroxide (1 mol L^{-1}) and the cathode, a piece of stainless steel net. The reaction was controlled at about 353 K; 0.1 A and continual agitation was necessary until the color of the solution in the anodic bath changed from orange to brick red. Then, the deposition was washed immediately with distilled water until no chloride ions were in the product. At last, the obtained composites were dried in vacuum drying oven at 333 K for 2 h.

The photo decolorization reactions of dye brilliant red ($C_{19}H_{10}Cl_2N_6Na_2O_2S_2$, X-3B) were carried out in a quartz reactor (Fig. 1), the initial concentration of the aqueous solution of X-3B was 50 mg L^{-1}, and the irradiation light source was a 375 W Iodine–Tungsten lamp with a wavelength range of 400–800 nm. Before irradiation the suspension was first stirred in the dark for 60 min to reach an equilibrated adsorption. The concentration of the copper element in the solution after photocatalytic reaction was detected by Inductively Coupled Plasma-Atomic Emission Spectrometry (ICP-AES).

3. Results and discussion

3.1. SEM morphology and surface characterization of nanoparticles

SEM images of the Cu_2O/chitosan nano-sized composites are shown in Fig. 2a and b.

Fig. 2a and b, the SEM images of CS particles, shows that the CS particles are irregularly shaped ones of about 100–500 nm in diameter; while in Fig. 2c, the SEM images of Cu_2O/CS composites, shows clearly that compared with the SEM images of pure CS nanoparticles, spindly Cu_2O nanoparticles are surrounded by a irregularly shaped CS

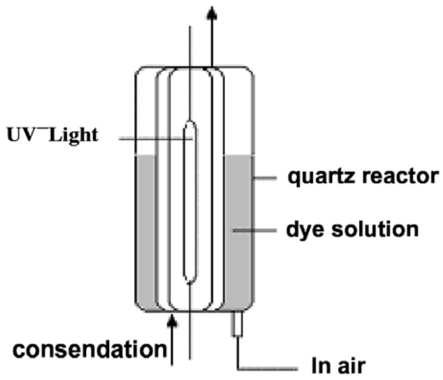

Fig. 1. The reactor of photocatalysis.

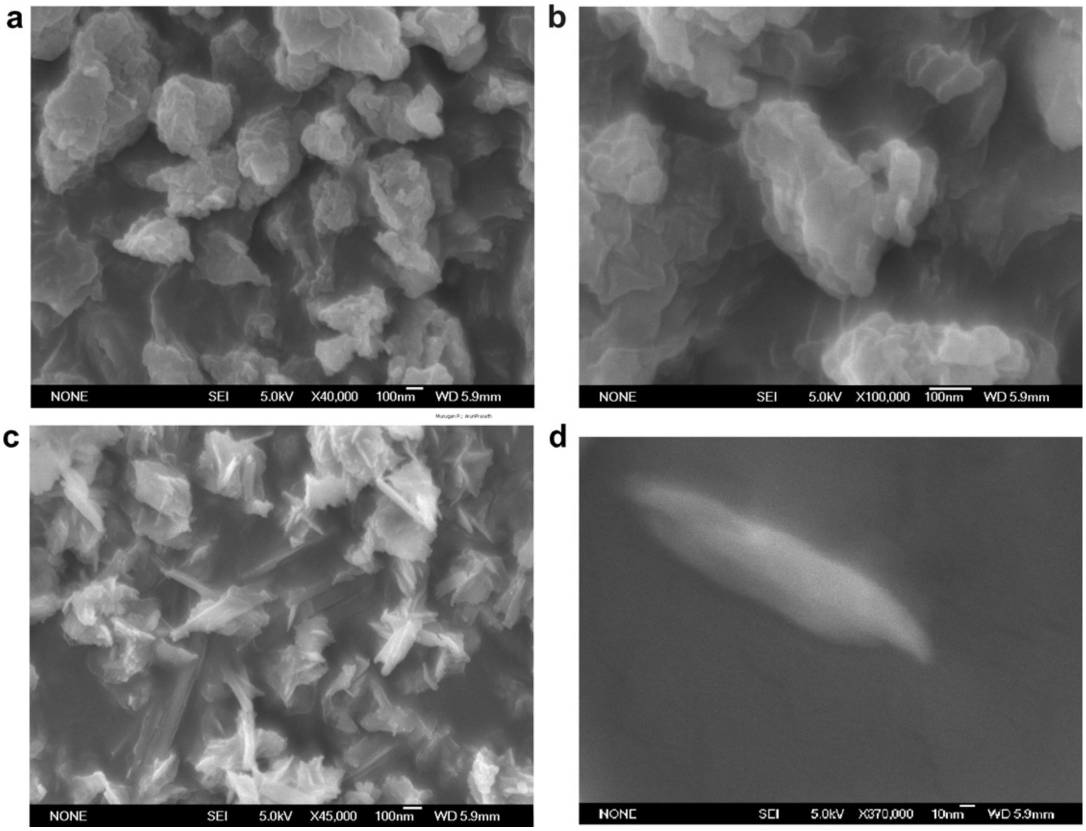

Fig. 2. (a) The SEM images of CS particles. (b) The SEM images of single CS nanoparticles. (c) The SEM images of Cu_2O/CS composites. (d) The SEM image of single Cu_2O nanocrystalline.

matrix. Fig. 2d was the SEM image of single Cu_2O nanocrystal. It was a spindle-shaped nanoparticle 30 nm in diameter and 150 nm in length which was accordance with the SEM of image in Fig. 2c.

3.2. The photocatalytic activities of Cu_2O/CS composites

A comparison of photocatalytic activities between Cu_2O and Cu_2O/CS composites is shown in Fig. 3. The suspension was first stirred in the dark for 2 h before irradiation. This was sufficient to reach an equilibrated adsorption as deduced from the steady-state concentrations. The result shows that Cu_2O/CS composites can enhance the photocatalytic activities of pure nano-sized Cu_2O in the degradation of dye brilliant red X-3B from 63% to 79%.

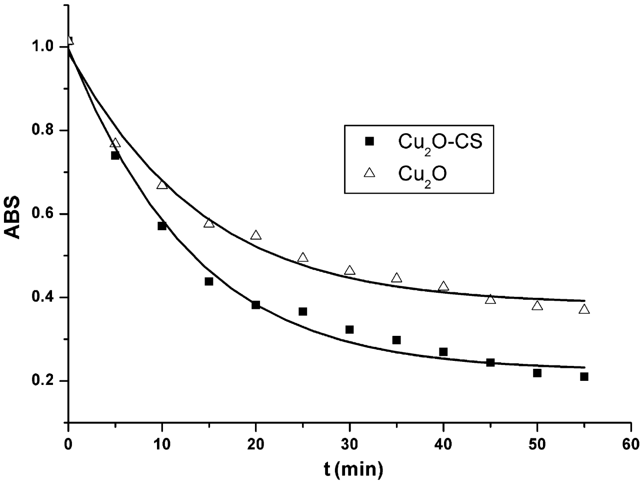

Fig. 3. Comparison of photocatalytic activities between pure Cu_2O and Cu_2O/CS composites under a visible light irradiation at $\lambda = 400$–800 nm. (The experiments were performed employing 500 mL of aqueous solutions containing 25 mg X-3B and 1 g L^{-1} of catalyst.)

The performances of Cu_2O/CS composites with variant mass ratios of Cu_2O in photocatalytic decoloration of reactive brilliant red X-3B were investigated under visible light irradiation. It's found that the highest degradation efficiency in the experiments is obtained when the composites contain 50 wt% Cu_2O, as shown in Fig. 4. When the mass ratio of Cu_2O in Cu_2O/CS composites is below 50 wt%, the catalytic efficiency is raised as the deposition of Cu_2O on CS increases; but it is raised slightly at higher Cu_2O loadings. The disappearance rate of X-3B by pure CS particles (contain 0 wt% Cu_2O in Fig. 4) was only about 15%, resulting from the decolorization of X-3B irradiated by light alone. The heterogeneous photocatalysis mainly occurred in molecule interfacial layers (Xie, Yuan, & Li, 2005), so the affinity adsorption properties between the reactants and photocatalyst surface play an important role in determining overall reaction rate (Chiou & Li, 2003; Hu, Wang, & Tang, 2001). X-3B is a strongly bound to the surface of Cu_2O/CS nanoparticles, which is ascribed to the NH_3^+

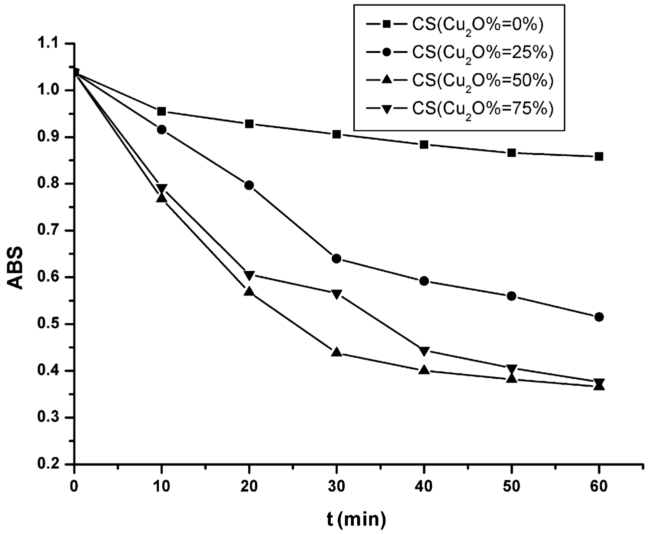

Fig. 4. Disappearance of X-3B by different mass ratio of Cu_2O in the Cu_2O/CS composites under a visible light irradiation at $\lambda = 400–800$ nm. (The experiments were performed employing 500 mL of aqueous solutions containing 25 mg X-3B and 500 mg L^{-1} of catalyst.)

ions with positive charges banded on the CS nanoparticles surface since anionic dye X-3B molecules have negative charges (Xie et al., 2005). So when Cu_2O increases, the binding of X-3B to Cu_2O/chitosan composites decreases because the cationic groups on CS are occupied by more Cu_2O molecules, although the Cu_2O concentration increases. For heterogeneous photocatalysis, surface absorption is the key step of the catalytic reaction, so the efficiency of photocatalytic decoloration of X-3B is reduced. Furthermore, when Cu_2O increases, the reaction solution turns brick red so that it is more difficult for visible lights to penetrate. So when the mass ratio of Cu_2O in Cu_2O/CS nanocomposites is higher than 50%, the adding of more Cu_2O will not increase the efficiency of photocatalytic degradation of X-3B substantially.

3.3. The concentration of residual copper ions

The concentration of copper element in water is a well-known issue which has to be controlled according to drinking water standard. One of the main reason why we selected CS as the carrier is that CS could eliminate copper element from the solution with chelation. In order to investigate the concentrations of residual copper element in the solution after the photocatalytic reactions, the solution system of Cu_2O/CS nanocomposites after photocatalytic degradation of X-3B with variant mass ratios of Cu_2O are measured by means of ICP-AES in the streams produced by once-through oxidation runs, as shown in Fig. 5.

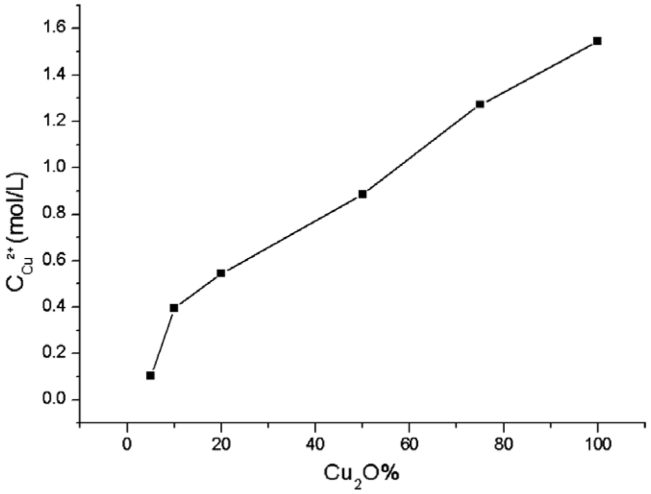

Fig. 5. The concentration of the copper element in the solution after photocatalysis reaction with different mass ratio of Cu_2O and Cu_2O/CS.

The results show that the concentrations of copper element decreases greatly after the depositing of Cu_2O on CS and it goes on decreasing as CS in Cu_2O/CS nanocomposites increases. As shown in Fig. 5, when the mass ratio of Cu_2O in Cu_2O/CS nanocomposites is lower than 50%, the residual concentration of copper element in the solution is lower than 1.0 mg L^{-1}, which is up to the WHOs drinking water standards in WHOs Guidelines for Drinking-water Quality. Taking the results of Fig. 4 into consideration, the best mass ratio of Cu_2O and the CS in the nano-sized Cu_2O/CS composites was 1:1 in consideration of the high photocatalytic efficiency and the controlling of the concentrations of copper element. But the valence state of copper can not be made certain by ICP methods, so we can not confirm the copper element was copper(I) or copper(II) on earth. We thought that some of the copper element in the solution may derive from Cu_2O nanocrystal that can not be combined firmly with CS carrier, or derive from the anodic photocorrosion of the Cu_2O nanocrystal during the photocatalysis reaction. All of the copper element which went into solution whether it was Cu_2O nanoparticles or Cu(II) ions could be detected as the residual copper concentration by ICP method.

4. Conclusions

Cu_2O/CS nanocomposites are prepared by electrochemical deposition. By the joint analysis of photocatalytic performance of Cu_2O/CS nanocomposites with variant mass ratios of Cu_2O in the decoloration of reactive brilliant red X-3B, and the chelation capability of CS, we find that when the mass ratio of Cu_2O in the Cu_2O/CS nanocomposites is 50%, the composites will provide us with a new feasibility to eliminate the pollutants by visible light irradiation in the advanced treatment of drinking water.

Acknowledgement

The work is financially supported by National Natural Science Foundation of China (No. 20207002).

References

Anpo, M., Matsuoka, M., Hanou, K., Mishima, H., Yamashita, H., & Patterson, H. H. (1998). The relationship between the local structure of copper(I) ions on Cu^+/zeolite catalysts and their photocatalytic reactivities for the decomposition of NO_x into N_2 and O_2 at 275 K. *Coordination Chemical Reviews, 171*, 175–184.

Bohannan, E. W., Shumsky, M. G., & Switzer, J. A. (1999). Epitaxial electrodeposition of copper (I) oxide on single-crystal gold (100). *Chemical Materials, 11*(9), 2289–2291.

Bordiga, S., Paze, C., Berlier, G., Scarano, D., Spoto, G., Zechina, A., et al. (2001). Interaction of N_2, CO and NO with Cu-exchanged ETS-10: a compared FTIR study with other Cu-zeolites and with dispersed Cu_2 O. *Catalysis Today, 70*, 91–105.

Chen, Jin-Yi, Zhou, Pei-Jiang, Li, Jia-Lin, & Li, Su-Qin (2007). Depositing Cu_2O of different morphology on chitosan nanoparticles. *Carbohydrate Polymers, 67*, 623–629.

Chiou, M. S., & Li, H. Y. (2003). Adsorption behavior of reactive dye in aqueous solution on chemical cross-linked chitosan beads. *Chemosphere, 50*, 1095–1105.

Chu, H. P., Lei, L., Hu, X., & Yue, P. L. (1998). Metallo-organic chemical vapor deposition (MOCVD) for the development of heterogeneous catalysts. *Energy & Fuels, 12*(6), 1108–1113.

Daltina, A.-L., Addadb, A., & Chopart, J.-P. (2005). Potentiostatic deposition and characterization of cuprous oxide films and nanowires. *Journal of Crystal Growth, 282*, 414–420.

Guido, R., Jacques, M., Michael, G., Nick, S., & Devendra, S. K. (1985). Charge carrier trapping and recombination dynamics in small semiconductor particles. *Journal of the American Chemical Society, 107*, 8054–8059.

Guzman, J., Saucedo, I., Revilla, J., Navarro, R., & Guibal, E. (2003). Copper sorption by chitosan in the presence of citrate ions: influence of metal speciation on sorption mechanism and uptake capacities. *International Journal of Biological Macromolecules, 33*, 57–65.

Hara, M., Hasei, H., Yashima, M., Ikeda, S., Takata, T., Kondo, J., et al. (2000). Mechano-catalytic overall water splitting (II) nafion-deposited Cu_2O. *Applied Catalysis A: General, 190*, 35–42.

Hu, Chun, Wang, Yizhong, & Tang, Hongxiao (2001). Influence of adsorption on the photodegradation of various dyes using surface bond-conjugated TiO_2/SiO_2 photocatalyst. *Applied Catalysis B: Environmental, 35*, 95–105.

Jorge, M.-V., Sergio, C., & Facundo, R. (2004). Formation of copper oxide films on fiberglass by adsorption and reaction of cuprous ions. *Thin Solid Films, 460*, 58–61.

Jorge, R. O., Tetsuya, O., Jorge, M. V., Ortiz, A., & Sofía, E. (2001). A catalytic application of Cu_2O and CuO films deposited over fiberglass. *Applied Surface Science, 174*, 177–184.

Li, J. L., Liu, L., Yu, Y., Tang, Y. W., Li, H. L., & Du, F. P. (2004). Preparation of highly photocatalytic active nano-size TiO_2–Cu_2O particle composites with a novel electrochemical method. *Electrochemistry Communications, 6*, 940–943.

Lu, Y. M., Chen, C. Y., & Lin, M. H. (2005). Effect of hydrogen plasma treatment on the electrical properties of sputtered N-doped cuprous oxide films. *Thin Solid Films, 480–481*, 482–485.

Marisa, M., Beppu, C., Arruda, E. J., Vieira, R. S., & Santos, N. N. (2004). Adsorption of Cu(II) on porous CS membranes, functionalized with histidine. *Journal of Membrane Science, 240*, 227–235.

Poizot, P., Laruelle, S., Grugeon, S., Dupront, L., & Taracon, J. M. (2000). Nano-sized transition-metal oxides as negative-electrode materials for lithium–ion batteries. *Nature, 407*, 496–499.

Quality Guidelines for Drinking-water Quality. Vol. 1:3rd ed. World Health Organization. (2004), p335.

Sahidi, F., Arachchi, J. K. V., & Jeon, Y. J. (1999). Food applications of chitin and chitosans. *Trends Food Science and Technology, 10*(2), 37–51.

Steenkamp, G. C., Keizer, K., Neomagus, H. W. J. P., & Krieg, H. M. (2002). Copper(II) removal from polluted water with alumina/chitosan composite membranes. *Journal of Membrane Science, 197*, 147–156.

Tang, Y., Chen, Z., Jia, Z., Zhang, L., & Li, J. (2005). Electrodeposition and characterization of nanocrystalline cuprous oxide thin films on TiO_2 films. *Materials Letters, 59*, 434–438.

Tsoncheva, T., Nickdov, R., Vankova, S., & Mehandjiev, D. (2003). CuO-activated carbon catalysts for methanol decomposition to hydrogen and carbon monoxide. *Canadian Journal of Chemistry, 81*, 1096–1100.

Vincendon, M. (1997). Regenerated chitin from phosphoric acid solutions. *Carbohydrate Polymers, 32*, 233–237.

Xie, Yibing, Yuan, Chunwei, & Li, Xiangzhong (2005). Photocatalytic degradation of X-3B dye by visible light using lanthanide ion modified titanium dioxide hydrosol system. *Colloids and Surfaces A: Physicochemical and Engineering Aspects, 252*, 87–94.

Yu, Y., Ma, L. L., Huang, W. Y., Li, J. L., Wong, P. K., & Yu, J. C. (2005). Coating MWNTs with Cu2O of different morphology by a polyol process. *Journal of Solid State Chemistry, 178*, 1488–1494.

Yu, Y., Du, F. P., Yu, J. C., Zhuang, Y. Y., & Wong, P. K. (2004). One-dimensional shape-controlled preparation of porous Cu_2O nano-whiskers by using CTAB as a template. *Journal of the Solid State Chemistry, 177*, 4640–4647.